Multiheterodyne Detection for Spectral Compression and Downconversion of Arbitrary Periodic Optical Signals

Josue Davila-Rodriguez, Marcus Bagnell, Charles Williams, *Student Member, IEEE*, and Peter J. Delfyett, *Fellow, IEEE, Fellow, OSA*

***Abstract*—Optical frequency combs are used as local oscillators for the measurement and analysis of unknown optical waveforms with periodic time domain structures. Experimental results obtained by heterodyning pulsed and phase-modulated laser sources are presented. The analysis is then extended to the heterodyning and sampling of bandlimited incoherent light sources. It is shown theoretically and experimentlly that the correlations between photodetected white light at different times can generate RF interference that is sensitive to the optical phase.**

***Index Terms*—Frequency combs, heterodyne.**

I. Introduction

SINCE its invention, the optical frequency comb [1]–[3], has been applied to several fields such as time and frequency metrology [4]–[6], length metrology [7], optical arbitrary waveform generation [8]–[11], and high precision spectroscopy [12]. All of these applications benefit from the fact that the frequency comb consists of a large set of coherent local oscillators with uniform frequency spacing. These oscillators can then probe the resonances of a molecular or atomic system in spectroscopic measurements, and become the Fourier basis whose amplitudes and phases are controlled for arbitrary waveform generation or provide the link between the optical frequency of a single combline and the microwave frequencies represented by the combline spacing in optical clocks.

Sampling electric fields directly at optical frequencies is practically an impossible task given the fact that the center frequency of the oscillation is well beyond the capabilities of electronic sampling devices. Notwithstanding, most optical signals contain information only within a small bandwidth (i.e., they are bandlimited). Heterodyning a high-frequency but bandlimited signal with a coherent oscillator produces an exact copy of the bandlimited signal centered at a frequency corresponding to the frequency difference between the coherent oscillator and the signal under test. This low-frequency copy can then be sampled by electronic means. This principle can be applied to optical signals, that is, a narrowband optical signal can be heterodyned with a continuous wave (CW) laser and sampled at the beat frequency. If the signal is distributed over periodically spaced portions of spectrum, it can be heterodyned with a set of coherent oscillators with a different frequency spacing to generate a series of beat notes in the RF domain that can then be sampled. Heterodyne techniques are useful because both amplitude and phase information are retained in the process. Some of the requirements for the local oscillators are frequency stability and a fixed phase relation between them, both of which are typically met by frequency comb sources.

Multiheterodyne detection with optical frequency combs was first proposed in [13] and has been implemented in a coherent configuration where two combs that share an optical reference are mixed and from the mixing products the effect of a medium on the signal comb can be deduced [7], [12], [14]. The mutual coherence of these combs makes possible the accumulation of signal over extended periods of time, beyond the coherence time of individual comblines.

In this paper, we utilize a frequency comb as a set of local oscillators to downconvert and sample periodic optical signals. The optical signals that are being sampled are not coherent with the local oscillator, which is a realistic approximation to measuring unknown optical signals as is the case in the spectral characterization of rapidly tunable CW lasers [15], mode-locked laser systems, and arbitrarily shaped optical waveforms. The most evident limitations are that the waveforms must have an underlying periodicity and that the lack of mutual coherence sets a limit on the maximum time over which signal can be accumulated. Three types of experiments are presented, wherein different types of sources are sampled: 1) pulses from an independent optical frequency comb source; 2) phase-modulated, CW light; and 3) periodically filtered, incoherent white light. In the first two experiments, the repetition rates are extremely detuned, by more than a multiple of the repetition rate of the lower repetition rate source and, therefore, the downconversion is performed using only a subset of the available comblines. An effective repetition rate detuning is introduced to accurately describe these experiments. In the third case, photocurrent interferometry of signals detected with time delays between them is performed to demonstrate the fidelity of the measurement.

The paper is organized as follows. In Section II, a conceptual description of the experiments is presented by considering the sources to have infinitely narrow (represented by Dirac delta functions) frequency components. Section III contains

Manuscript received April 11, 2011; revised July 25, 2011; accepted August 05, 2011. Date of publication August 18, 2011; date of current version October 05, 2011.

The authors are with the Center for Research and Education in Optics and Lasers, The College of Optics and Photonics, University of Central Florida, Orlando, FL 32816 USA (email:josue@creol.ucf.edu; mbagnell@creol.ucf.edu; charles@creol.ucf.edu; delfyett@creol.ucf.edu).

Color versions of one or more of the figures in this paper are available online at http://ieeexplore.ieee.org.

Digital Object Identifier 10.1109/JLT.2011.2165315

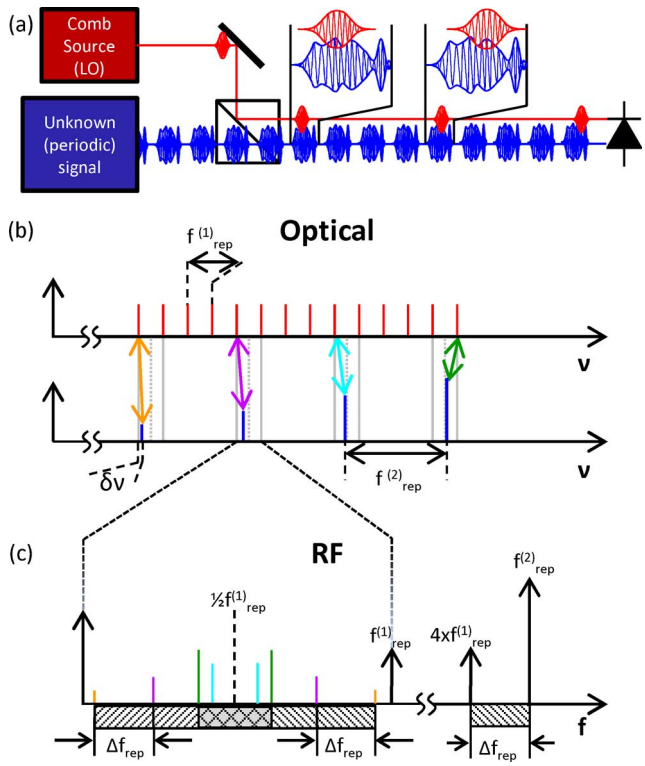

Fig. 1. Conceptual picture of the multiheterodyne detection with a large repetition rate detuning. (a) Time domain depiction of the process. Notice the pulse walk-off between the LO and the signal under test. (b) Frequency domain picture in the optical domain and (c) the photodetected spectrum of the superposition of the two optical combs. The highest frequency combline pair (green) illustrates the aliasing effect. This is illustrated by the shaded areas underneath the frequency axis as well, with an overlapping region. Also note the difference in scales between the optical and RF frequency axes.

the experimental results in three separate sections, the first including the results of the mixing products between two mutually incoherent mode-locked laser combs, the second between a mode-locked comb and phase-modulated CW light and, finally, the derivations and experimental results for spectral interferometry of downconverted white light. Conclusions are presented in Section IV.

II. Conceptual Description

Equivalent time and frequency domain pictures can be drawn to explain the phenomena at hand. A conceptual form of the experimental setup is shown in Fig. 1, where one of the sources is an optical frequency comb and the other is the source under test. For this description, we shall assume that the source under test is a frequency comb with narrow components whose amplitudes and phases are unknown. This assumption is valid as long as the observation time does not exceed the coherence time, which can be on the order of hundreds of microseconds to milliseconds for free-running, narrow-linewidth lasers [16], while cavity stabilized lasers have reached the sub-hertz linewidth regime [17]–[19], allowing for second-long observation times.

In reference to Fig. 1(a), the source under test is depicted to have a repetition rate that is equal to four times that of the LO plus a small additional detuning. This additional detuning determines the rate at which the waveforms "walk" through each other, generating a slowly varying interference pattern which repeats itself at a rate equal to the difference between the repetition rate of the source under test and the closest harmonic of the repetition rate of the LO.

From the frequency domain picture [see Fig. 1(b) and (c)], it can be readily seen that the RF beat notes will appear at the frequency difference between each pair of comblines. The effective repetition rate detuning determines the rate at which the comblines from each source walk-off from each other, thus determining the beat-note spacing in the RF domain. It should be noted that for large detuning or a large interacting bandwidth, the beat notes may get to the point where the next closest combline is not to the lower frequency side but to the higher frequency side. When this occurs, a different set of beat notes with the same spacing but at an overall offset will appear within the band of interest, generating a signal with a slower overall periodicity (aliased). To avoid this problem the following limit must be satisfied:

$$N \times |\Delta f_{\text{rep}}| + \delta\nu < \frac{1}{2} f_{\text{rep}}^{(1)}. \tag{1}$$

In this expression, N is the number of interacting comblines, $\Delta f_{\text{rep}} = f_{\text{rep}}^{(2)} - \text{Round}(f_{\text{rep}}^{(2)}/f_{\text{rep}}^{(1)}) \times f_{\text{rep}}^{(1)}$ is the effective repetition rate detuning, $f_{\text{rep}}^{(2)}$ is the larger of the two repetition rates, and $\delta\nu$ is the frequency difference between the two closest comblines. From (1), we can see that there is a tradeoff between the maximum repetition rate detuning and the available interacting bandwidth. The frequency difference of the two closest comblines also affects the maximum usable bandwidth and, in some cases, it can be tuned to a convenient value by changing the carrier-envelope offset frequency of the reference comb. For example, assume $f_{\text{rep}}^{(1)} = 1$ GHz and $f_{\text{rep}}^{(2)} = 4.01$ GHz, then $\lfloor f_{\text{rep}}^{(2)}/f_{\text{rep}}^{(1)} \rfloor = 4$ and the beat-note spacing $\Delta f_{\text{rep}} = 4.01\ \text{GHz} - 4 \times 1\ \text{GHz} = 10$ MHz. A maximum of 50 beat notes can be observed within the band from dc to $f_{\text{rep}}^{(1)}/2 = 500$ MHz, which limits the optical bandwidth that can be used before aliasing effects appear to a maximum of 200 GHz.

The equivalent time domain picture is that of a sampling gate that has variable delay with respect to the periodic signal under test, given by the pulse walk-off. The relative position of the pulses/waveforms comes back to its original position after a time equal to $1/\Delta f_{\text{rep}}$, which in turn gives rise to the beat-note spacing in the RF domain.

It is important to note that this is a linear technique and, consequently, the interacting quantities are the electric fields. The resulting waveforms arise from electric field interference, which, if the local oscillator is properly characterized, gives a snapshot of the periodic signal under test, including the carrier under the envelope.

This process achieves two independent forms of spectral conversion: 1) it downconverts the carrier frequency from the optical domain to the RF domain; and 2) it compresses the spectrum by reducing the "empty" spaces in between comblines from the original repetition rate to the new sampled rate, given by the repetition rate detuning. The downconversion factor can be defined as the carrier optical frequency divided by the carrier microwave frequency and the compression factor as the ratio of the original repetition rate to the sampled repetition rate.

As the repetition rate detuning is reduced, the generated waveforms have a longer periodicity. This detuning must evidently reach a point where the periodicity is longer than the coherence of the sources. In the frequency domain, this can be thought of as an overlap between finite-linewidth components (as opposed to the ideal delta-like components described so far) when the spectral compression is carried beyond the linewidth of individual comblines. A more detailed analysis is presented later in this paper (see Section III-C) as an introduction to the periodically filtered white light experiments, but it must be stated that a lower limit to the repetition rate detuning can be written as

$$\Delta f_{\mathrm{rep}} > \Delta \nu_{\mathrm{LW}} \tag{2}$$

where $\Delta \nu_{\mathrm{LW}}$ is the parameter that represents the linewidth of the individual comblines and its definition may vary depending on the particular application.

III. Experiments

The experiments presented cover various cases for which multiheterodyning an unknown, periodic, optical signal with a frequency comb is useful as a means to downconvert and sample the electric fields. Although all the experiments are conceptually very similar, in practice, they represent a broad set of cases. For this reason, the metrics for evaluation of the performance of the experimental setups are chosen specifically for each of the experiments. In some cases, the availability of different diagnostic tools also determines the type of analysis that can be performed.

Section III-A deals with pairs of optical frequency comb sources generated from mode-locked lasers. Section III-B deals with a mode-locked laser comb that samples phase-modulated CW light and Section C includes experiments done with periodically filtered white light.

A. Mode-Locked Laser Comb Sources

In the first experiment, an erbium-doped fiber passively mode-locked laser source is used as a local oscillator to sample the electric field from a semiconductor-based harmonically mode-locked laser, locked to an intracavity Fabry–Pérot etalon (FPE)[20]. The repetition rates of the lasers are ∼250 MHz and ∼10.24 GHz, respectively. The detuning is extremely large and only the beat notes from the 250 MHz spaced comblines that are nearest to the 10 GHz spaced comblines are used in the measurement, yielding an effective repetition rate detuning of ∼600 kHz, which is calculated by comparing the 41st harmonic of the fiber laser with the fundamental of the 10.24 GHz comb source. This is equivalent to sampling one out of every forty-one 10.24 GHz repetition rate pulses on each cycle.

Optical and RF spectra of the results are shown in Fig. 2. An effort was made in this experiment to make the detuning large enough to almost fill the available RF bandwidth (1/2 of 250 MHz) for one copy of the spectrum. The absolute position of the downconverted comb can also be controlled by varying the carrier-envelope offset frequency of the 250 MHz comb. A smaller span of the RF measurement shows clearly resolved beat notes in Fig. 2(c). The interacting bandwidth is essentially

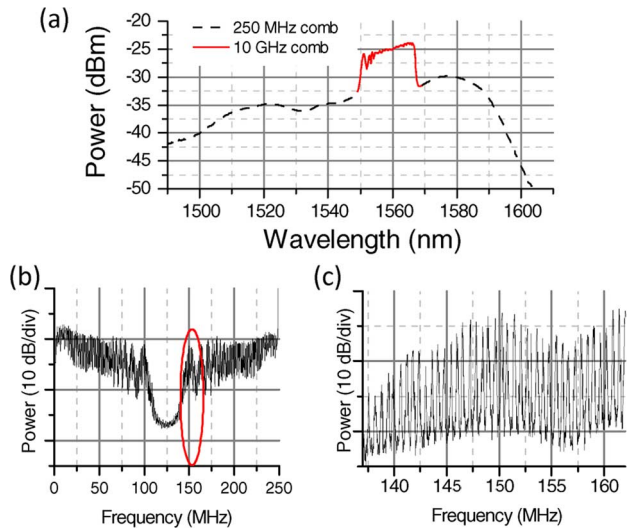

Fig. 2. (a) Optical spectra of the mode-locked comb sources. (b) Photodetected RF spectrum. (c) Smaller span of the RF spectrum.

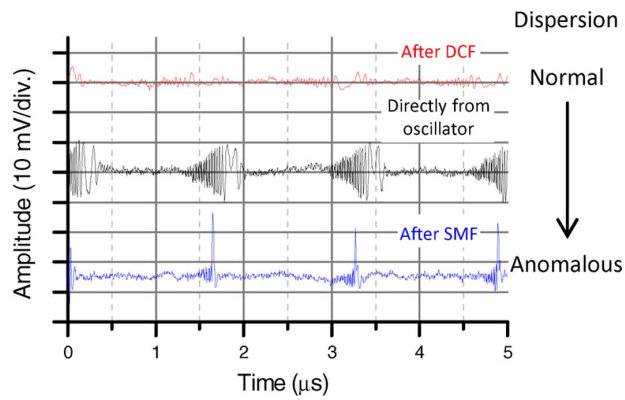

Fig. 3. Time domain RF waveforms after downconversion as the 10.24 GHz mode-locked comb experiences different amounts of dispersion.

the optical bandwidth of the semiconductor mode-locked laser which is ∼2.12 THz, that is, more than 200 comblines. The downconversion factor $(\nu_{\mathrm{opt}}/f_{\mathrm{RF}})$ is on the order of 3×10^6, and the compression factor $(\Delta\nu_{\mathrm{opt}}/\Delta f_{\mathrm{RF}})$ is $\sim 17 \times 10^3$.

In order to test whether the spectral phase information is preserved, the photodetected signal is low pass filtered (ideally with a filter that cuts off everything above 125 MHz, but in this case, the oscilloscope bandwidth was limited to 80 MHz) and the resulting waveform is sampled with an electrical oscilloscope. The semiconductor laser's pulses are then passed through different amounts of dispersion (∼100 m of standard single-mode fiber with $D \approx 17$ ps/nm/km and a few meters of dispersion compensating fiber with $D \approx -170$ ps/nm/km). The results are shown in Fig. 3, where it can be observed that as the pulse chirp, and hence, the spectral phase of the optical signal is varied, the chirp and pulse duration of the RF signal varies accordingly.

It is interesting to note in Fig. 3 that the sampled pulses coming straight from the laser cavity are chirped as expected from a semiconductor laser. The sharp rise in the front edge and the long tail are evidence of residual third-order phase. The RF carrier in these waveforms is chirped, mirroring the optical carrier of the mode-locked pulses, because the sampled RF

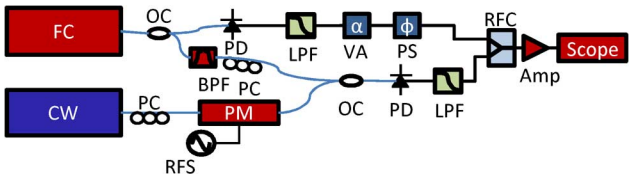

Fig. 4. Experimental setup. Amp: amplifier, BPF: bandpass filter, FC: frequency comb, CW: CW laser, LPF: low-pass filter, OC: optical coupler, PC: polarization controller, PD: photodetector, PM: phase modulator, PS: phase shifter, RFC: RF coupler, RFS: RF synthesizer, VA: variable attenuator.

waveforms contain information about the instantaneous optical frequency.

The measurements presented in this section give a good picture of the spectral intensity of the target comb. The spectral phase is preserved relative to the reference comb. As long as the reference comb has a flat phase profile over the interacting bandwidth, the sampled waveform represents the target E-field accurately. Knowledge of the absolute frequency of each combline would require resolving the combline number ambiguity from the reference comb. That is, knowledge of the absolute frequency of the reference comb combined with the ability to trace the unique RF beats of each combline pair yields the absolute frequency of the target comblines. This issue has also been addressed in [15] for the measurement of the absolute frequency of CW lasers by using two reference frequency combs with detuned repetition rates. The sensitivity of our measurement is ultimately limited by the length of time over which a signal can be accumulated due to the lack of coherence between the target and reference combs.

B. Phase Modulated CW Light

Another particular case of interest is that of phase-modulated CW light. In fact, recent work [15] has been done in the measurement of the absolute frequency of rapidly tuned CW lasers. The lack of intensity fluctuations and the fact that there is only a slow change in optical frequency make it an interesting case to test some of the limits of the technique. For example, the small number of interacting comblines reduces the number of free parameters and it is therefore easier to fully characterize the experimental data by fitting the measured waveform to an expected theoretical waveform.

The experimental setup is shown in Fig. 4. As in the previous experiment, the same commercially available, 250 MHz, erbium-fiber frequency comb is used as a local oscillator in this experiment to downconvert the comb generated by phase modulation at 10.006 31 GHz of CW light from a commercially available CW laser. In order to fully recover the comb parameters, it is desirable to obtain a high-fidelity sampled electrical waveform. Besides careful low-pass filtering to avoid higher frequency components to leak into the sampling device, good suppression of the 250 MHz tone from intracomb beatings is imperative to best use the available resolution of the sampling device. For this reason, an interferometric carrier suppression arm is used, as shown in Fig. 4. Additional filtering can be done in the digital domain after the data have been recorded.

The optical spectrum of both sources is shown in Fig. 5(a), and the photodetected RF spectrum is shown in Fig. 5(b). Notice

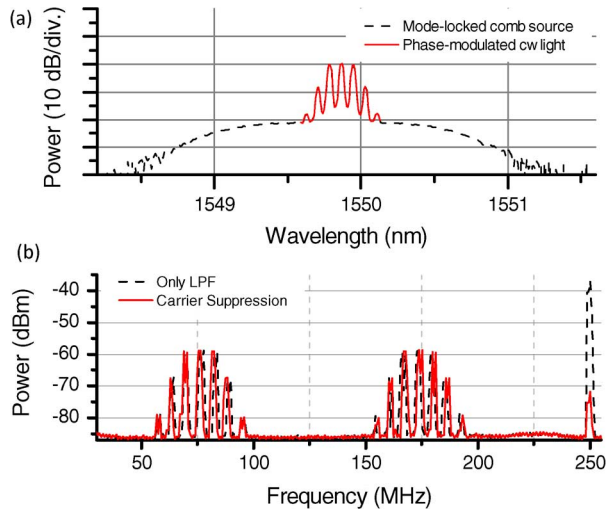

Fig. 5. (a) Optical spectra of the phase-modulated CW light and the reference comb. (b) Photodetected RF spectrum.

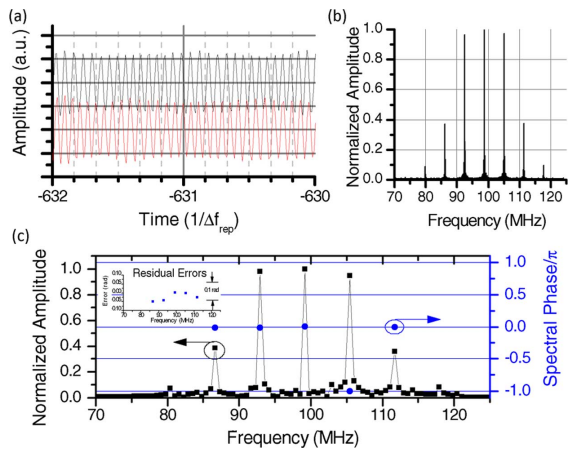

Fig. 6. (a) Time domain waveforms, the red trace is displaced $\sim 1/2$ a period with respect to the black trace. (b) FFT of the full waveform. (c) FFT and spectral phase of a 1.6 μs segment of the waveform. A constant offset and a linear trend have been removed from the phase plot. Only the phase values where the FFT has significant power are shown. The inset plot shows the errors of the phase compared to the theoretically expected values.

the difference in the 250 MHz carrier suppression through the interferometric filtering.

A real-time high bandwidth oscilloscope was used to record waveforms obtained from the multiheterodyne beat notes. After filtering the beat notes between 70 and 120 MHz, an example of the obtained waveform is shown in Fig. 6 with a time-shifted (by $\sim 1/2$ of a period of the repetition rate detuning) version of the same waveform shown in the red trace to show that the frequency modulation of the waveform can be observed by inspection. The repetition rate detuning was $\sim$6.31 MHz and $\sim$1262 cycles of this waveform were recorded in this case. The time axes can be conveniently normalized to the repetition period. A Fourier transform of the entire dataset is shown in Fig. 6(b). Fig. 6(c) shows the Fourier transform of a 1.6 μs segment of the sampled signal. The spectral phase of this fast Fourier transform (FFT) is available as well and shown in the figure after removing a constant offset and a linear trend. Notice that the expected π phase shift between the ± 1 comblines. The spectral phase can

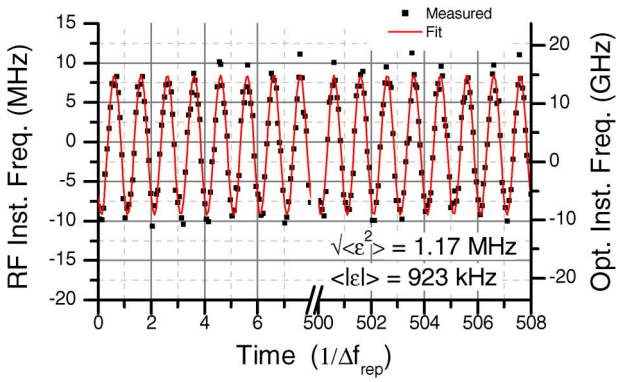

Fig. 7. Instantaneous frequency of the photodetected waveform. RF on the left y axis and optical in the right axis. Notice the compression between the two scales. The rms and mean absolute error are indicated in the figure. The fit errors are ∼5% of the full range.

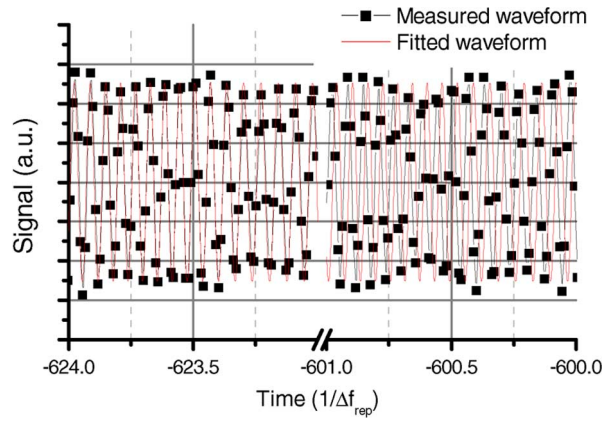

Fig. 8. Fitted time domain waveform. Notice that after a carrier frequency shift and bandwidth decompression, this corresponds exactly to the phase-modulated optical waveform.

only be recovered from a shorter time segment of the signal because of the free-running nature of the target comb with respect to the LO comb, which causes the signal to add incoherently for time spans longer than the inverse of the linewidth of the comb teeth.

The phase of the optical field changes periodically with time. The phase of the downconverted RF waveform is expected to change in the same way. There is an additional slowly varying phase factor that undergoes a random walk and it represents the phase between the local oscillator modes and the CW laser (ϕ_0). This can be observed when the signal is recorded for times longer than the inverse of the individual combline linewidth. The phase of the photodetected RF waveform will then have a time dependence given by

$$\phi(t) = \beta \sin(2\pi \Delta f_{\rm rep} t + \phi_M) + \phi_0. \tag{3}$$

Interestingly, while the phase ϕ_0 undergoes a random walk, its *derivative* has zero mean, and therefore, the frequency modulation of the waveform is notaffected by this term beyond a zero-mean random quantity. That is, $f(t) = (1)/(2\pi)(d\phi)/(dt) = \Delta f_{\rm rep}\beta\cos(2\pi\Delta f_{\rm rep}t + \phi_M) + \phi_0'$, and $\langle\phi_0'\rangle \sim 0$.

The recorded time domain data can be analyzed in several ways. For example, from the previous RF spectrum (and knowledge of the ratio of Bessel functions), the depth of phase modulation index can be estimated at ∼1.4 rad. Another way of measuring such modulation index is through a time domain analysis of the instantaneous frequency of the measured waveform. Fig. 7 shows the measured instantaneous frequency and a calculated sinewave at the phase modulation frequency of the RF waveform (equal to the repetition-rate detuning) where only the phase factor ϕ_M was fit to the data. Notice that the sinewave does not go out of step with the frequency modulation even after hundreds of periods (Fig. 7 shows 510 periods or ∼80 μs). This is due to the fact that the optical phase drops out of the frequency modulation calculation and thus, the random walk that the relative phase between both lasers undergoes does not affect the measurement. The repetition rate detuning between the waveforms gives the compression factor, which can be used to calculate the instantaneous optical frequency of the phase-modulated light, shown in the right y axis of Fig. 7.

The complete signal can be fit to a perfect phase-modulated waveform only for short time intervals, as the relative phase between the lasers undergo a random walk and, after several periods, the waveforms slowly go out of step. Fig. 8 shows this effect, where a perfect phase-modulated sinewave was fit in a portion of the waveform and then followed several periods in time. After ∼20 periods (∼3.2 μs), the phase of the waveform is visibly changed. This is consistent with the linewidth of the local oscillator comblines, which is >100 kHz.

C. Periodically Filtered White Light

When the source under test is a bandlimited white light source, the corresponding electric fields can be represented through a Fourier expansion whose frequency component spacing depends inversely on the observation time. A classical analysis for the correlations between two delayed copies of a white light signal is developed by Hanbury Brown and Twiss. [21]. In this paper, a heterodyne version of the derivation is presented for a single combline, but the conclusions can be extended to the multi-combline beating by superposing individual solutions.

An advantage of using heterodyne detection to downconvert a white light spectrum is that the resulting photocurrent interferometry has extremely high resolution, limited only by the available RF spectrum analyzers. As a comparison, a typical grating-based optical spectrum analyzer can resolve fringes with a resolution on the order of 1 GHz, while a RF spectrum analyzer could potentially resolve spectral fringes with spacing smaller than 1 Hz. The power spectral density of the white light spectrum then becomes the ultimate limitation in the detectability of the fringes.

1) Theory and Simulations: A few assumptions must be stated first: 1) The white light is considered band-limited; 2) the local oscillator is assumed to be coherent (i.e., a delta-like function); and 3) the frequency difference between the local oscillator and the closest nonzero frequency component of the white light is larger than the white light bandwidth. This allows us to treat the white light homodyne beats independently from the heterodyne beats. The assumptions are not extremely constraining, provided careful filtering.

A random but bandlimited optical field is considered in this derivation. In general, the spectrum of a bandlimited signal may consist of a finite number of sparsely located finite bandwidth peaks. If such a random electric field is observed for a finite time τ, then it can be represented by a Fourier series in the following form:

$$E_{\mathrm{ASE}}(t) = 2\sum_{n=n_0}^{n=n_0+N} |q_n| \cos\left[\frac{2\pi n}{\tau}t + \phi_n\right] \quad (4)$$

where the coefficients q_n are related to the integrated optical power in the nth frequency bin and are nonzero only for a finite frequency range, $\nu_{\min} < n/\tau < \nu_{\max}$. ϕ_n are the phases of the frequency components and are assumed to be uniformly distributed over the range $[0, 2\pi]$. As shown in the analysis in [21], the photocurrent generated by such a field is given by

$$i(t) = \mathcal{R}\langle P_{\mathrm{ASE}}\rangle + 2\mathcal{R}\sum_{n>m}\sum_{m}\sqrt{P_n}\sqrt{P_m} \times \cos\left[\frac{2\pi}{\tau}(m-n)t + (\phi_m - \phi_n)\right] \quad (5)$$

where $\mathcal{R}$ is the photodetector responsivity, $\langle P_{\mathrm{ASE}}\rangle$ is the average power contained in the signal, and P_n and P_m are the average powers contained in the nth and mth frequency bins, respectively. The photocurrent fluctuations represented by the second term in (5) average zero, but, nonetheless, they can be shown to be correlated to the signals detected at a time delay Δt_A. The case that is of interest to us in this paper is a heterodyne version of this experiment. The total electric field obtained by adding a CW carrier to a random signal like the one in (4) is given by

$$E_{\mathrm{tot}}(t) = 2A\cos[2\pi\nu_L t + \phi_c] + 2\sum_{n}|q_n|\cos\left[\frac{2\pi n}{\tau}t + \phi_n\right]. \quad (6)$$

The photodetected signal has four main components: the two terms in (5) plus an additional average power due to the local oscillator and a heterodyne term. As long as care is taken to keep the frequency difference between the local oscillator and the center of the white light's spectrum larger than the white light bandwidth, the heterodyne term can be filtered and observed independently in the RF domain. The voltage across a resistor R_L of the heterodyne part of the photodetected signal is given by

$$V^{(1)}(t) = \mathcal{R}R_L\sqrt{P_L}\sum_{n}\sqrt{P_n} \times \cos\left[2\pi\left(\frac{n}{\tau} - \nu_L\right)t + (\phi_n - \phi_c)\right]. \quad (7)$$

After including delays at different positions (see Fig. 9) at the second photodetector, the voltage is

$$V^{(2)}(t) = \mathcal{R}R_L\sqrt{P_L}\sum_{n}\sqrt{P_n} \times \cos\left[2\pi\left(\frac{n}{\tau} - \nu_L\right)t + (\phi_n - \phi_L) + \frac{2\pi n}{\tau}\Delta t_A - 2\pi\nu_L\Delta t_L\right]. \quad (8)$$

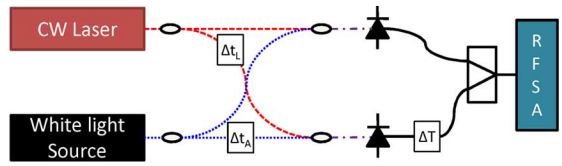

Fig. 9. Conceptual experimental setup for white light photocurrent interferometry.

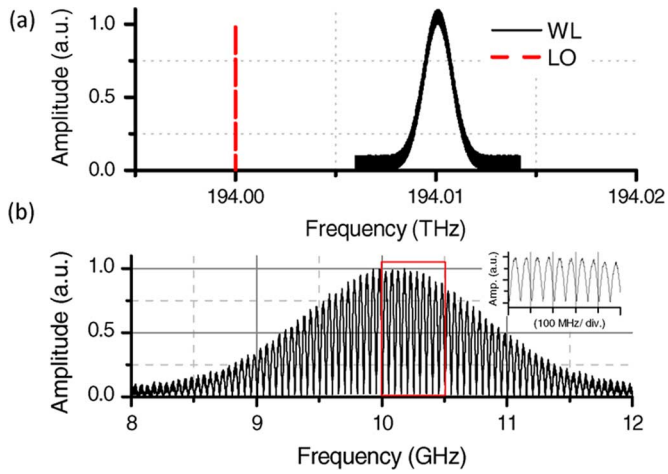

Fig. 10. Simulation results. (a) Optical spectra. (b) Photocurrent interference for a fixed 20 ns delay.

Note that phase delays in the optical paths (Δt_A and Δt_L) change the phase of the photodetected spectrum directly. If we add the signals $V^{(1)}$ and $V^{(2)}$ in an RF coupler as shown in Fig. 9, the interference pattern will have a fringe spacing related to the accumulated delay between the white light paths, but the fringe position will be extremely sensitive to small path changes in the order of the wavelength of light, due to the phase factor $((2\pi n)/(\tau)\Delta t_A - 2\pi\nu_L\Delta t_L)$. The expression for the spectral interference is given by

$$\left|\mathcal{F}\left\{\frac{1}{2}\left(V^{(1)}(t) + V^{(2)}(t)\right)\right\}\right| = \cos\left[2\pi\left(\frac{n}{\tau} - \nu_L\right)\Delta T + 2\pi\frac{n}{\tau}\Delta t_A - 2\pi\nu_L\Delta t_L\right] \times \tilde{V}^{(1)}\left(\frac{n}{\tau} - \nu_L\right) \quad (9)$$

where $\tilde{V}^{(1)}((n)/(\tau) - \nu_L)$ is the Fourier transform of the signal in a single channel. Notice that n/τ and ν_L are optical frequencies. As a consequence, while the *periodicity* of the interference pattern changes with the difference frequency $(n/\tau - \nu_L)$, its *phase* (the absolute position of the fringes in the RF spectrum) is sensitive to delays (Δt_A) smaller than the wavelength of light.

Fig. 10 shows a numerical calculation of the interference in the RF spectral domain of a heterodyne white light signal. Fig. 10(a) shows the optical spectra, with the CW laser in red and the white light modeled with a random amplitude variations on top of a Gaussian spectrum and uniformly distributed random spectral phases. The interference pattern for a path delay ($\Delta t_A = 20$ ns) is shown in Fig. 10(b).

2) Experimental Results: Several experiments have been performed to test the idea behind the previous section and we intend to expand upon them elsewhere.

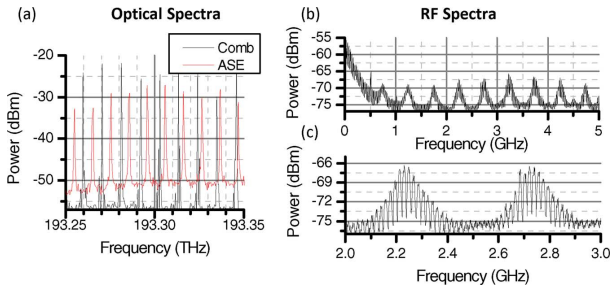

Fig. 11. Multiheterodyne white light interferometry. (a) Optical spectra of the periodically filtered white light (blue) and the mode-locked laser (red). (b) RF spectra of the interfering photocurrents of the downconverted white light.

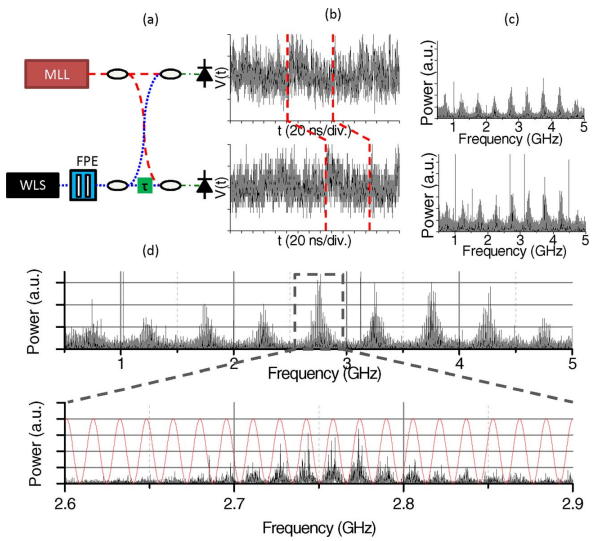

Fig. 12. Spectral interference of downconverted incoherent light. (a) Experimental setup. (b) Sampled RF waveforms. (c) Power spectra of the sampled waveforms. (d) Spectral interference with superposed transfer function of a spectral interferometer (red).

As a proof that the concept can be applied to a multiheterodyne version of the experiment, a periodically filtered white light source was generated by taking amplified spontaneous emission (ASE) from a semiconductor optical amplifier and filtering it with a FPE, followed by amplification stages to boost the power in each transmitted resonance. The FPE has 10.24 GHz of free-spectral range and a finesse of ∼100, making the width of each resonance of ∼100 MHz. An actively, harmonically mode-locked laser where comb operation was forced by CW optical injection, such as the one described in [22], was used to downconvert this white light spectrum. The repetition rate detuning was carefully adjusted to have a clear separation between resonances in the RF domain. The optical spectra of the sources are shown in Fig. 11(a), where a clear walk-off can be seen between the peaks. The photodetected signals were then interfered in the RF domain, generating a series of periodically spaced RF peaks, each with an interference pattern imposed upon it, as shown in Fig. 11(b) and (c).

An experiment was performed where the photocurrents were electronically sampled independently and then interfered. The results are shown in Fig. 12. A delay of ∼12 m of fiber was added between the two arms and the waveforms sampled in

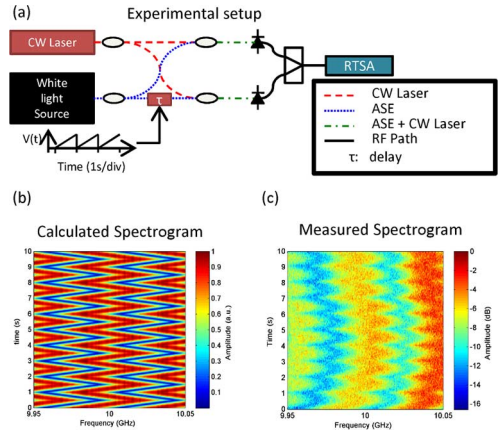

Fig. 13. Heterodyne photocurrent interferometry. (a) Experimental setup. (b) Calculated interferometry spectrogram. (c) Measured interferogram.

two independent channels of a high-bandwidth oscilloscope. The sampled waveforms are shown in Fig. 12(b). Note that while each of the waveforms contains essentially only noise (incoherent), the two waveforms appear remarkably similar and are highly correlated with a delay of ∼63 ns. The FFT spectra of these signals are shown in Fig. 12(c). When the signals are added, spectral interference can be observed in each of the downconverted ASE peaks. Fig. 12(d) shows the resulting interference. The transfer function of a spectral interferometer is shown in red in the smaller span plot for visual aid.

Since the interference pattern is sensitive to small path length deviations, another test was made where a single ASE peak and a CW laser were used to measure the spectrogram of the interference while the optical path in one of the arms of the interferometer was driven by a piezo-electric fiber stretcher, as shown in Fig. 13(a). The spectrogram in Fig. 13(b) is obtained by calculating the interference pattern while a slow triangular modulation is imposed on Δt_A. The function driving Δt_A is a 1 Hz triangular wave with a peak-to-peak amplitude of 4 fs. That is, the path delay between the two ASE paths is only changed by 4 fs ($\Delta t_A = 20\,\text{ns} \pm 2\,\text{fs}$) or, close to a single cycle of a 200 THz carrier. The experimentally obtained spectrogram is shown in Fig. 13(c), where a clear periodic shift in the fringes is observed with a frequency of 1 Hz.

IV. Conclusion

In conclusion, we have shown a series of experiments where the use of a comb source as a local oscillator to downconvert and compress optical signals is desirable. We have provided examples with coherent (too narrowband to be observed in short observation times) sources where we have compressed the spectrum of phase modulated light waveforms by factors of $\sim 1600\times$ and mode-locked pulses by $\sim 17000\times$. The carrier frequencies were downconverted from the ∼200 THz regime to the microwave regime ∼100 MHz. An analysis is presented for white light heterodyne detection and interferometry. Interference patterns akin to those of spectral interferometry can be obtained in the microwave regime by adding the photocurrents. In this fashion, an extremely high-resolution version of white light spectral interferometry can be performed.

REFERENCES

[1] J. Ye and S. Cundiff, *Femtosecond Optical Frequency Comb: Principle, Operation, and Applications*. New York: Springer Verlag, 2005.

[2] R. Holzwarth, T. Udem, T. Hänsch, J. Knight, W. Wadsworth, and P. Russell, "Optical frequency synthesizer for precision spectroscopy," *Phys. Rev. Lett.*, vol. 85, no. 11, pp. 2264–2267, Sep. 2000.

[3] S. A. Diddams, L.-S. Ma, J. Ye, and J. L. Hall, "Broadband optical frequency comb generation with a phase-modulated parametric oscillator," *Opt. Lett.*, vol. 24, no. 23, pp. 1747–1749, Dec. 1999.

[4] T. Udem, J. Reichert, R. Holzwarth, and T. W. Hänsch, "Accurate measurement of large optical frequency differences with a mode-locked laser," *Opt. Lett.*, vol. 24, no. 13, pp. 881–883, Jul. 1999.

[5] S. Diddams, D. Jones, J. Ye, S. Cundiff, J. Hall, J. Ranka, R. Windeler, R. Holzwarth, T. Udem, and T. Hansch, "Direct link between microwave and optical frequencies with a 300 THz femtosecond laser comb," *Phys. Rev. Lett.*, vol. 84, no. 22, pp. 5102–5105, May 2000.

[6] T. Udem, R. Holzwarth, and T. W. Hänsch, "Optical frequency metrology," *Nature*, vol. 416, no. 6877, pp. 233–237, Mar. 2002.

[7] I. Coddington, W. C. Swann, and N. R. Newbury, "Coherent linear optical sampling at 15 bits of resolution," *Opt. Lett.*, vol. 34, no. 14, pp. 2153–2155, Jul. 2009.

[8] N. K. Fontaine, D. J. Geisler, R. P. Scott, T. He, J. P. Heritage, and S. J. B. Yoo, "Demonstration of high-fidelity dynamic optical arbitrary waveform generation," *Opt. Exp.*, vol. 18, no. 22, pp. 22988–22995, Oct. 2010.

[9] P. Delfyett, S. Gee, H. Izadpanah, S. Ozharar, F. Quinlan, and T. Yilmaz, "Optical frequency combs from semiconductor lasers and applications in ultrawideband signal processing and communications," *J. Lightw. Technol.*, vol. 24, no. 7, pp. 2701–2719, Jul. 2006.

[10] Z. Jiang, D. S. Seo, D. E. Leaird, and A. M. Weiner, "Spectral line-by-line pulse shaping," *Opt. Lett.*, vol. 30, no. 12, pp. 1557–1559, Jun. 2005.

[11] M. Akbulut, S. Bhooplapur, I. Ozdur, J. Davila-Rodriguez, and P. J. Delfyett, "Dynamic line-by-line pulse shaping with GHz update rate," *Opt. Exp.*, vol. 18, no. 17, pp. 18284–18291, 2010.

[12] I. Coddington, W. C. Swann, and N. R. Newbury, "Coherent multiheterodyne spectroscopy using stabilized optical frequency combs," *Phys. Rev. Lett.*, vol. 100, p. 013902, 2008.

[13] S. Schiller, "Spectrometry with frequency combs," *Opt. Lett.*, vol. 27, no. 9, pp. 766–768, May 2002.

[14] F. Ferdous, D. E. Leaird, C.-B. Huang, and A. M. Weiner, "Dual-comb electric-field cross-correlation technique for optical arbitrary waveform characterization," *Opt. Lett.*, vol. 34, no. 24, pp. 3875–3877, Dec. 2009.

[15] F. R. Giorgetta, I. Coddington, E. Baumann, W. C. Swann, and N. R. Newbury, "Fast high-resolution spectroscopy of dynamic continuous-wave laser sources," *Nat. Photonics*, vol. 4, no. 12, pp. 853–857, 2010.

[16] I. Ozdur, M. Akbulut, N. Hoghooghi, D. Mandridis, S. Ozharar, F. Quinlan, and P. J. Delfyett, "A semiconductor-based 10-GHz optical comb source with sub 3-fs shot-noise-limited timing jitter and ∼500-Hz comb linewidth," *IEEE Photon. Technol. Lett.*, vol. 22, no. 6, pp. 431–433, Mar. 2010.

[17] A. D. Ludlow, X. Huang, M. Notcutt, T. Zanon-Willette, S. M. Foreman, M. M. Boyd, S. Blatt, and J. Ye, "Compact, thermal-noise-limited optical cavity for diode laser stabilization at $1 \times 10(-15)$," *Opt. Lett.*, vol. 32, no. 6, pp. 641–643, Mar. 2007.

[18] Y. Y. Jiang, A. D. Ludlow, N. D. Lemke, R. W. Fox, J. A. Sherman, L.-S. Ma, and C. W. Oates, "Making optical atomic clocks more stable with 10–16-level laser stabilization," *Nat. Photonics*, vol. 5, pp. 158–161, Jan. 2011, .

[19] B. Young, F. Cruz, W. Itano, and J. Bergquist, "Visible lasers with subhertz linewidths," *Phys. Rev. Lett.*, vol. 82, no. 19, pp. 3799–3802, May 1999.

[20] F. Quinlan, S. Ozharar, S. Gee, and P. J. Delfyett, "Harmonically mode-locked semiconductor-based lasers as high repetition rate ultralow noise pulse train and optical frequency comb sources," *J. Opt. A: Pure Appl. Opt.*, vol. 11, no. 10, p. 103001, Oct. 2009.

[21] R. H. Brown and R. Q. Twiss, "Interferometry of the intensity fluctuations in light. I. Basic theory: The correlation between photons in coherent beams of radiation," in *Proc. Roy. Soc. A: Math., Phys. Eng. Sci.*, Nov. 1957, vol. 242, no. 1230, pp. 300–324.

[22] C. Williams, F. Quinlan, and P. Delfyett, "Injection-locked mode-locked laser with long-term stabilization and high power-per-combline," *IEEE Photon. Technol. Lett.*, vol. 21, no. 2, pp. 94–96, Jan. 2009.

Author biographies not included at author request due to space constraints.